LEFT VENTRICLE SEGMENTATION WITH MIXTURE OF GAUSSIAN ACTIVE CONTOURS

Xiaoxu Wang, Qingmao Hu

Human Computer Interaction Centre,
Shenzhen Institute of Advanced Technology,
1068 Xueyuan Ave., Xili, Shenzhen,
Guangdong, 518055, P. R. China

Pheng Ann Heng

Virtual Reality, Visualization and
Imaging Research Centre,
Department of Computer Science and Engineering,
The Chinese University of Hong Kong,
Shatin, N.T., Hong Kong

ABSTRACT

Cine MRI is an imaging technique for visualizing the left ventricle wall motion in a heart beating cycle. The paper proposed a method to semi-automatically segment the left ventricle (LV) boundaries from a stack of cine MRI and build a LV mesh. The different intensities in the MRI are modeled with the mixture of Gaussian method. The thresholds between them are semi-automatically determined by K-means initialization and the expectation maximization (EM) method. The spatial constrain is added into the model with active contour models, which fit explicit contours on the boundary of the area of interest. We propose a marching cube alike initialization method of the active contour models. A 3D mesh is built from a stack of contours and smoothed afterwards. Stroke volume, myocardium mass and ejection function can be estimated from the LV boundary mesh and the endocardium mesh.

Index Terms— Cine MRI, left ventricle reconstruction, mixture of Gaussian, marching cube, active contour models

1. INTRODUCTION

Magnetic Resonance Imaging is a technology of imaging the internal organs with the resonance of hydrogen nuclei. The hydrogen nuclei are rotating in the same direction in magnetic field. When excited with an electric current in the orthogonal direction with certain frequency, the rotation hydrogen nuclei will deviate from the previous rotation direction. After removing the electric current, the rotated nuclei will come back to the old rotation direction and emit a signal with the same frequency as the input signal. In a uniform magnetic field, the rotation speed of hydrogen nuclei depends on the magnitude of the magnetic field. In a gradient magnetic field, protons in the nuclei rotate in gradient speed. A MRI machine can image different location of human body. The left ventricle wall has darker intensities in MRI and is comparatively easy to be segmented from the blood pool. With the mixture of Gaussian and deformable models, the left ventricle boundaries of a stack of short axis (SA) MRI are segmented and tesselated to an endocardial surface and an epicardial surface. The left ventricle myocardium mass, stroke volumes and the ejection fraction can be measured and compared to the ground truth provided by experienced cardiologists. Used alone or coupled with blood flow simulation as in [1], the method would help with diagnosis and research on left ventricle malfunctions of such as ischemia or hypertrophy.

Stroke volume and ejection fraction are interested in cardiac dysfunction diagnosis. Much effort has been put on the left ventricle reconstruction from MRI or CT data with deformable models. Shi et. al, 2000 [2] introduced a left ventricular cavity surface reconstruction from medical images. After the contours segmented from each image slice, denauly tessellation and local smoothing method are apply to get a triangular surface of the left ventricle. Zhang et. al 2007 [3] proposed a FEM based left ventricular motion estimation. A geodesic approach for shape-driven and tracking of left ventricles is proposed in Paragios, 2002 [4]. The mixture of Gaussian model can also provide image forces for the level set method [5] [6]. Kaus et. al, 2003 [7] automatically segment the left ventricle boundaries with deformable models, and also demonstrate that 3D mesh can be built from MRI.

The data comes from Sunnybrook Helth Sciences Centre, Canada, as the data for LV segmentation challenge in MICCAI09. Six to twelve SA images were obtained from the atrioventricular ring to the apex.

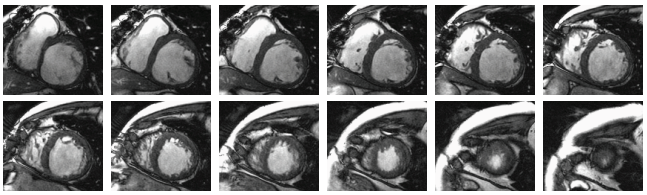


Fig. 1. 12 SA MRI from the left ventricle base to the apex

This paper presents a cine MRI segmentation method with mixture of Gaussian models and active contour models. Two 3D triangular meshes on endo-surface and epi-surface of the left ventricle are tessellated from a set of 2D contours on MRI. Segmentation and reconstruction methods are illustrated in Section 2. Results are presented in Section 3.

2. METHODS

Segmentation of the left ventricle is a difficult task due to a few anatomical factors. The proximity between the endocardial wall and papillary muscles poses difficulty in separating them solely with intensity based segmentation methods. Active contour models represent the boundary of an object as a deformable contour with elasticity. With good initialization, they would deform to fit the left ventricle cavity. A few initialization methods and forces have been proposed for deforming active contour models to fit the LV cavity. Active contour models are pulled with balloon forces[8] or distance map image forces[9]. The magnitude of balloon force is difficult to set considering the stop criteria. Distance map image forces are less reliable when the contour is pulled near a edge with discontinuity. With semi-automatic mixture of gaussian method, the LV myocardium intensity area is detected and a contour is initialized with marching cube [10] alike method. The similar intensities of the lung and right ventricular (RV) insertion points would cause the ambiguity in epicardial border detection. A deformable model with spatial and shape constraints yields more robust result.

2.1. Thresholding with Mixture of Gaussian

Detection of the left ventricle cavity boundary is a feasible task because it has good contrast in the MRI. The cardiac MRI can be clustered into three areas only based on intensities. The area with light intensity has lung bronchus, heart blood pool, fat. Another area has muscles include the myocardium. The lung area has dark intensity. The histogram of the MRI can be modeled with mixture of three Gaussian models. By approximating the Gaussian model parameters with expectation maximization method, the parameters for thresholding three intensity areas can be automatically estimated.

Assume the intensities in a image is a probability distribution. Each point has probability $p(x)$ to have intensity x. We model each intensity cluster as a gaussian distribution given a prior. The probability of a point with intensity x in a cluster j is

$$p(x_j) = -\frac{1}{\sqrt{2\pi}\sigma} exp(-\frac{\|x-\mu_i\|^2}{2\sigma_j^2}). \quad (1)$$

.

The prior of each intensity area $p(j)$ is estimated with K-means. In E-step, each step a point is clustered to the nearest center. In M-step, the center of every clusters are reestimated. The posterior distribution of being in a cluster $p(j|x)$ can be calculated with Bayes rules

$$p(j|x) = p(x|j)p(j)/\sum_{j=1}^{M} p(x|j)p(j), \quad (2)$$

with $p(x|j)$ calculated in equation 1. The point with intensity x can be clustered into group j with $max_j p(j|x)$.

In the mixture of Gaussian method, the mean μ_i and variance σ_i of each cluster, as in equation 1, are estimated with expectation maximization method. In the expectation step, the activation is calculated with current parameters of each cluster, as in equation 1. The posterior of a point with intensity x is then calculated with equation 2 and the gaussian distribution parameters are reestimated. In the maximization step, the prior of each cluster and the parameters of each Gaussian distribution are calculated. The new prior of each cluster equal to the sum of probability of points with any intensity belong to this cluster.

$$p(j) = \sum_x p(j|x) \quad (3)$$

The average value of each cluster is

$$\mu_j = \sum_x xp(x|j). \quad (4)$$

The variance of each cluster can be calculated with

$$\sigma_j^2 = E(\|x-\mu_j\|^2) = \sum_x \|x-\mu_j\|^2 p(x|j). \quad (5)$$

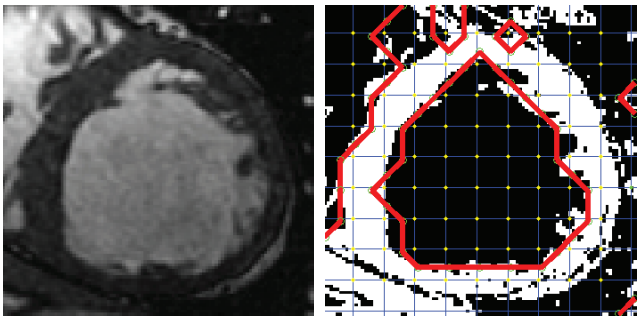


Fig. 2. A middle ventricle slice in the middle of systole shown in the left figure. The binary image after thresholding and marching cube initialization is shown in the right figure.

Coupled with spatial information, three areas with different model of intensities are partitioned with mixture of Gaussian models. The area of left ventricle muscle is selected for the next-step segmentation. The binary image of a middle ventricle slice in the middle of systole after thresholding is shown in Figure 2.

2.2. Segmentation with Active Contour Models

Active contour models [11] with gradient image forces work well when the initialized contour is near the boundary. Automatic initialization in the region of interest would work when the image forces near the edges can be brought to the rest of image, such as gradient vector flow (GVF) [12]. We propose for an active contour automatic initialization method which

initializes the contour near the boundary with a marching cube [10] alike method. The object can be identified in a binary map. The task is to get an explicit contour near the boundary in the binary map. The first step is to divide the binary image into small grids. A line with end vertices in the middle of the grid cube edge is inserted into a list. The binary value of four corners of each cube determine which kind of line is inserted. There are 16 different cases if not combined because of symmetry or isomorphism. In Figure 3, four cases in the first pattern when the black vertex rotate. Similarly, four cases in the second pattern, and four cases in the third pattern. Two different cases in the last pattern considering different color of the center point, and two other cases if switching black and white points.

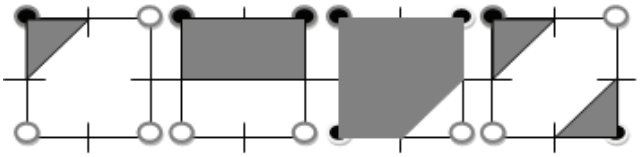


Fig. 3. A total of 16 cases of line insertion to thresholded binary images.

In Figure 2, marching cube lines are inserted between the muscle area and the blood pool area. The lines are connected into arcs. One of the longest connected lines with minimum radius variance is picked as the ventricle cavity contour. The active contour is initialized with this contour. The energy function of active contour models has two terms, internal energy and image gradient forces. The gradient of the binary image is used as external forces. The minimum change of the slope and curvature in neighboring arcs is taken as the internal constraint.

$$\begin{aligned} \alpha x_{ss} + \beta x_{ssss} + \frac{\partial I}{\partial x} = 0 \\ \alpha y_{ss} + \beta y_{ssss} + \frac{\partial I}{\partial y} = 0 \end{aligned} \tag{6}$$

As in a closed contour, the first vertex and the end vertex are defined at the same vertex. Let $v(0) = v(n)$. The derivatives are approximated with a finite difference. The equation 6 can be turned into

$$\begin{aligned} \alpha(v_i - v_{i-1}) - \quad & \alpha(v_{i+1} - v_i) \\ & +\beta[v_{i-2} - 2v_{i-1} + v_i] \\ & -2\beta[v_{i-1} - 2v_i + v_{i+1}] \\ & +\beta[v_i - 2v_{i+1} + v_{i+2}] \\ & +(f_x(i), f_y(i)) = 0 \end{aligned} \tag{7}$$

The coefficient matrix on the contour vertices is precalculated. The image forces on the contours are updated each step as the contour moves. The active contour is iteratively deforming and fitting the boundary until the internal forces is balanced with external forces. Weights on different energy can be adjusted to fit the contour better.

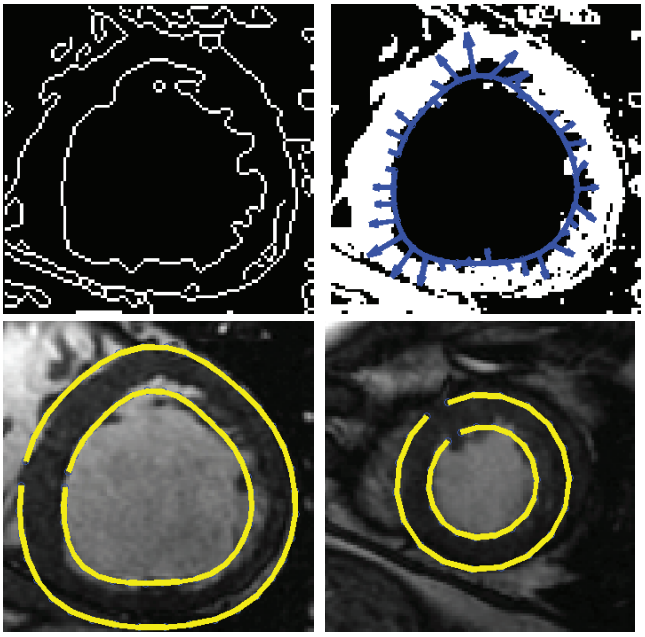


Fig. 4. Left up figure is obtained by canny edge detector. Right up figure shows the image forces on an active contour.Left bottom image is the active contour model segmentation result of a middle ventricle image. Left right image is the segmentation result of a slice near the apex.

In Figure 4, the ventricle cavity boundary is selected from the canny edge detector results. This edge is sensitive to the threshold selection and artifacts, and cannot tell the difference between the papillary muscles and myocardium. Therefore it is usually not used as segmentation results. Intensity gradient is calculated from the mask created by the ventricle cavity boundary, and used as image forces for active contour models. The image forces on the contour can be viewed in Figure 4. The segmentation result of a middle ventricle slice and a slice near the apex is shown in 4.

2.3. LV Boundary Reconstruction

The lateral bifurcation between the left ventricle and the right ventricle can be taken as anatomical feature. A set of active contours on the boundaries of a stack of MRI, which start from the lateral bifurcation, are tesselated to a hemisphere LV boundary with triangular elements. There are 12 slices SA MRI from the LV base to the apex. The distance between two parallel SA MRI is 8mm. The reconstructed LV boundary is accurate enough to measure the ejection function, stroke volume and the myocardium mass.

3. RESULTS

A left ventricle boundary reconstructed from MICCAI challenge 2009 data are shown in Figure 5.

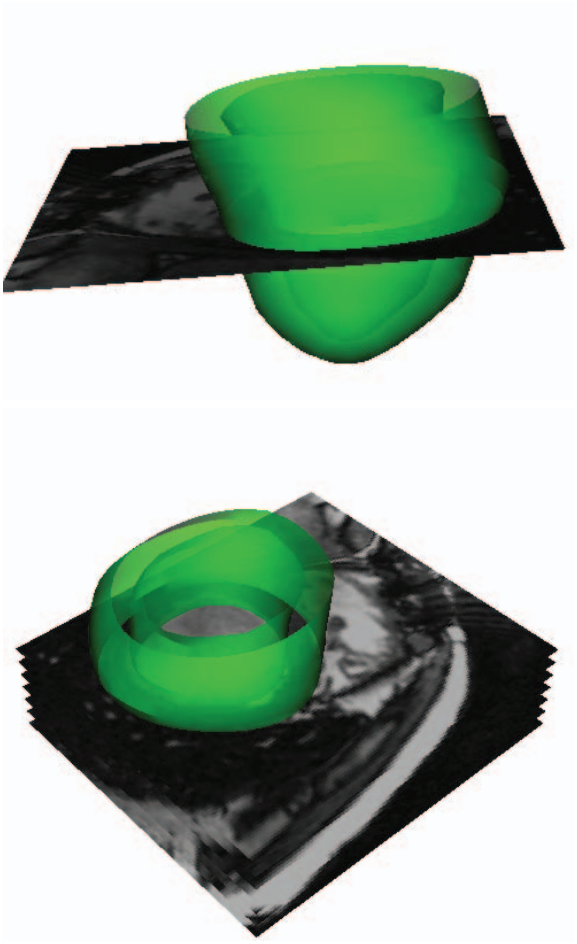


Fig. 5. 3D reconstruction results from Cine MRI. A long axis view and a view showing that it is reconstructed from a stack of short axis MRI.

Endocardial and epicardial contours were compared with manually segmented results in multiple slices at the end of diastole (ED) and the end of systole (ES) phases, following the convention of including papillary muscles and endocardial trabeculae in the ventricular cavity. Given normalized false positive area (NFPA) as (false positive area) / (labeled ground truth area) and normalized false negative area (NFNA) as (false negative area) / (labeled ground truth area), values in the table are the average values of multiple slices at left ventricle base, middle ventricle and apex.

Left ventricle contour segmentation results are robust with about 3% error on middle ventricle endocardium boundary. Middle ventricle false positive error and false negative error are smaller than errors at the LV base and the apex.

	ES	ES	ED	ED
	NFPA	NFNA	NFPA	NFNA
Base	0.106	0.076	0.131	0.107
Middle Ventricle	0.037	0.033	0.115	0.027
Apex	0.16	0.19	0.112	0.018

Fig. 6. Table: Validation of the segmentation results on manually segmented ground truth.

4. REFERENCES

[1] S. Kulp, M. Gao, S. Zhang, Z. Qian, S. Voros, D. Metaxas, and L. Axel, "Using high resolution cardiac ct data model and visualize patient-specific interactions between trabeculae and blood flow," *in Proceeding of Medical Image Computing and Computer Assisted Intervention*, 2011.

[2] P. Shi, A. J. Sinusas, R. T. Constable, E. L. Ritman, and J. S. Duncan, "Point-tracked quantitative analysis of left ventricle surface motion from 3d image sequences," *IEEE Transactions on Medical Imaging*, vol. 19(1), pp. 36–50, 2000.

[3] H. Zhang, S. Tong, H. Liu, and P. Shi, "Simultaneous recovery of left ventricular motion and input forces from medical image sequences," *in Proceeding of International Symposium on Biomedical Imaging*, pp. 380–383, 2007.

[4] N. Paragios, "A level set approach for shape-driven segmentation and tracking ofthe left ventricle.," *IEEE Transactions on Medical Imaging*, vol. 22(6), pp. 773–776, 2003.

[5] G. Dharanibai and J. P. Raina, "Gaussian mixture model based level set technique for automated segmentation of cardiac mr images," *International Journal of Engineering Science and Technology*, vol. 3, pp. 2970–2976, 2011.

[6] Zhenping Xie, Shitong Wang, and Dewen Hu, "New insight at level set & gaussian mixture model for natural image segmentation," *Signal, Image and Video Processing*, pp. 1–16, 2011.

[7] M. R. Kaus, J. Von Berg, J. Weese, W. Niessen, and V. Pekar, "Automated segmentation of the left ventricle in cardiac mri," *Medical Image Analysis*, vol. 8(3), pp. 245–254, 2004.

[8] L. D. Cohen, "On active contour mod," *Computer Vision, Graphics, and Image Processing: Image Understanding*, vol. 53(2), pp. 211–218, 1989.

[9] X. Huang and D. Metaxas, "Metamorephs: Deformable shape and appearance models.," *IEEE Transactions on Pattern Analysis and Machine Intelligence*, vol. 30, pp. 1444–1459, 2009.

[10] W. E. Lorensen and H. E. Cline, "Marching cubes: A high resolution 3d surface construction algorithm," *Computer Graphics (Proceedings of SIGGRAPH)*, vol. 21(4), pp. 163–169, 1987.

[11] M. Kass, A. Witkin, and D. Terzopoulos, "Snakes: Active contour models," *International Journal of Computer Vision*, pp. 321–331, 1988.

[12] C. Xu and J. L. Prince, "Snakes, shapes, and gradient vector flow," *IEEE Transactions on Image Processing*, vol. 7(3), pp. 359–369, 1998.